Chinese Chemical Letters 36 (2025) 110468

Contents lists available at ScienceDirect

Chinese Chemical Letters

journal homepage: www.elsevier.com/locate/cclet

Swelling and erosion assisted sustained release of tea polyphenol from antibacterial ultrahigh molecular weight polyethylene for joint replacement

Yue Ren[a,*], Kang Li[a], Yi-Zi Wang[a], Shao-Peng Zhao[a], Shu-Min Pan[a], Haojie Fu[c], Mengfan Jing[a], Yaming Wang[a], Fengyuan Yang[b,*], Chuntai Liu[a,*]

[a] State Key Laboratory of Structural Analysis, Optimization and CAE Software for Industrial Equipment, National Engineering Research Center for Advanced Polymer Processing Technology, Zhengzhou University, Zhengzhou 450002, China
[b] Tianjian Laboratory of Advanced Biomedical Sciences, Academy of Medical Sciences, Zhengzhou University, Zhengzhou 450000, China
[c] Department of Stomatology, The First Affiliated Hospital of Zhengzhou University, Zhengzhou 450000, China

ARTICLE INFO

Article history:
Received 31 July 2024
Revised 12 September 2024
Accepted 14 September 2024
Available online 15 September 2024

Keywords:
Tea polyphenol
Antibacterial
PEO
UHMWPE
Joint replacement

ABSTRACT

The considerable hazard posed by periprosthetic joint infections underlines the urgent need for the rapid advancement of *in-situ* drug delivery systems within joint materials. However, the pursuit of sustained antibacterial efficacy remains a formidable challenge. In this context, we proposed a novel strategy that leverages swelling and erosion mechanisms to facilitate drug release of drug-loaded ultrahigh molecular weight polyethylene (UHMWPE), thereby ensuring its long-lasting antibacterial performance. Polyethylene oxide (PEO), a hydrophilic polymer with fast hydrating ability and high swelling capacity, was incorporated in UHMWPE alongside the antibacterial tea polyphenol (epigallocatechin gallate, EGCG as representative). The swelling of PEO enhanced water infiltration into the matrix, while the erosion of PEO balanced the release of the encapsulated EGCG, resulting in a steady release. The behavior was supported by the EGCG release profiles and the corresponding fitted release kinetic models. As demonstrated by segmented antibacterial assessments, the antibacterial efficiency was enhanced 2 to 3 times in the PEO/EGCG/UHMWPE composite compared to that of EGCG/UHMWPE. Additionally, the PEO/EGCG/UHMWPE composite exhibited favorable biocompatibility and mechanical performance, making it a potential candidate for the development of drug-releasing joint implants to combat prosthetic bacterial infections.

Periprosthetic joint infection (PJI) is a catastrophic complication after orthopedic joint replacement associated with reinfection, reoperation, and high mortality [1-3]. According to the Australian Orthopaedic Association National Joint Replacement Registry (AOANJRR), multiple revisions for PJI in joint replacement have shown continued growth in the last 5 years, reaching 6.8% procedures in 2022 [4]. Patients suffering from PJI may experience mild to severe symptoms, including joint swelling, purulence or sinus tract accompanied by fever for acute infections and persistent pain for chronic infections [5]. Although systemic antibiotic therapy is broadly applied, treatment for staphylococcal infections lasts 6–8 weeks and, in some cases, extends up to 5 years [6]. This prolonged duration is due to the limited and ineffective bioavailability of a wide range of antibiotics at the bone/implant interface [7,8]. To enhance patients' quality of life and reduce healthcare costs, it is imperative to develop *in situ* drug-releasing antibacterial joint materials.

Ultrahigh molecular weight polyethylene (UHMWPE) bearing surfaces are articulating components of joint prostheses with excellent self-lubrication and mechanical properties [9,10]. Two predominant methodologies are employed to endow UHMWPE joint materials with antibacterial performance. One is to modify the surface with drug-carrying pores and coatings. Lahiri *et al.* engineered gentamicin-loaded micron-sized pores on the surface of UHMWPE by solvent etching, lyophilization and vacuum impregnation technique. The modified surface of UHMWPE showed potential against bacterial infection through the release of gentamicin [11,12]. Porous coatings introduced on UHMWPE liners through electrostatic spray were able to load and release more gentamicin, as confirmed by the release profile and 10 days of antibacterial testing [13]. Another direct approach is to blend drugs in UHMWPE. The entire UHMWPE matrix could serve as a reser-

* Corresponding authors.
E-mail addresses: renyue@zzu.edu.cn (Y. Ren), yangfy_zzu@outlook.com (F. Yang), ctliu@zzu.edu.cn (C. Liu).

https://doi.org/10.1016/j.cclet.2024.110468
1001-8417/

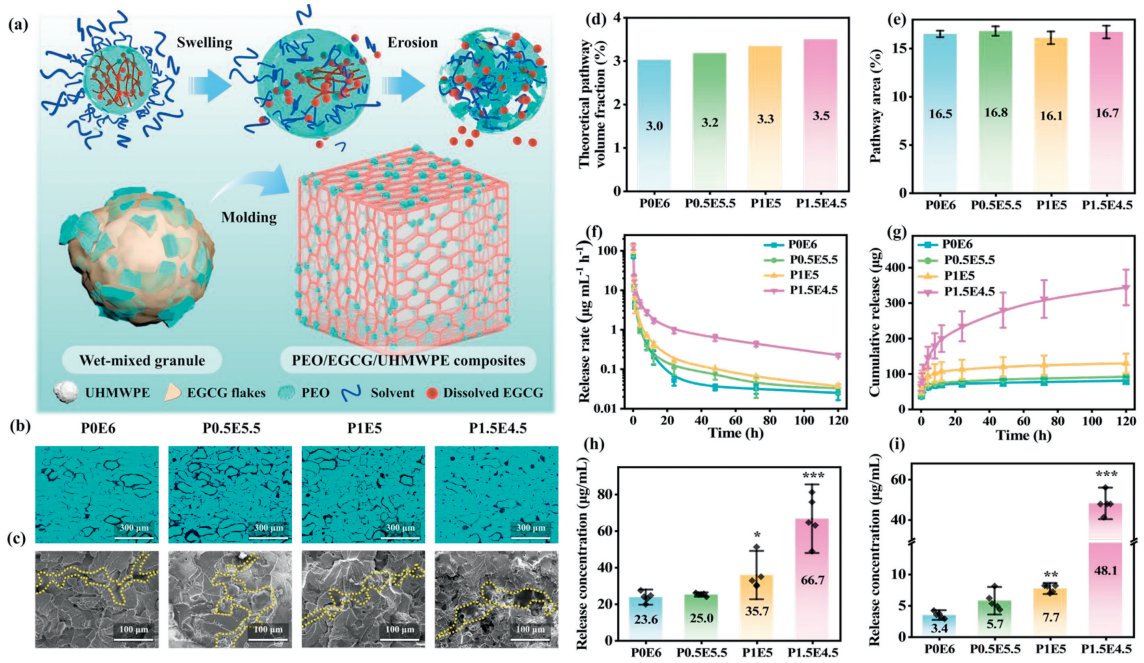

Fig. 1. Preparation and characterization of PEO/EGCG/UHMWPE composite. (a) Schematic illustration of the preparation process and release mechanism of PEO/EGCG/UHMWPE composite. (b) OM images of the cut slices. (c) SEM images of the cryo-fractured surface. The yellow dot line in SEM images refers to the delivery pathways in the composite. (d) Theoretical pathway volume fraction of PEO/EGCG/UHMWPE composites. (e) Hybrid pathway area conducted from OM images. (f) EGCG release rate and (g) cumulative EGCG release profiles of PEO/EGCG/UHMWPE composites. EGCG release concentration of PEO/EGCG/UHMWPE composites at a total release duration of (h) 12 h and the following (i) 108 h. Data are presented as mean ± standard deviation (SD) ($n = 5$). $^{*}P < 0.05$, $^{**}P < 0.01$, $^{***}P < 0.001$ *vs.* P0E6.

voir to carry drugs stably, exerting longer antibacterial duration than drug-loaded pores and coatings [14-16]. A variety of antibiotics (including gentamicin, tobramycin, ciprofloxacin, levofloxacin, vancomycin, linezolid, colistin, and rifampicin) were incorporated into UHMWPE, rendering the antibiotic-releasing UHMWPEs effective against the causative PJI pathogens for over 3 weeks [17]. To circumvent antibiotic-resistant bacteria, we introduced tea polyphenol-releasing UHMWPE as an alternative to antibiotic therapy. The incorporated tea polyphenols formed continuous delivery pathways in UHMWPE matrix at the concentration of 6 wt%, endowing the material with 100% antibacterial effect on *Staphylococcus aureus* (*S. aureus*) and *Escherichia coli* (*E. coli*) [18-21]. Furthermore, oxidation stability and crosslinking of UHMWPE were improved by tea polyphenols. Despite the progress for drug-releasing UHMWPE, it remains a great challenge in achieving sustained drug release to match the acute and chronic infection cycle.

In recent years, a multitude of methodologies has emerged for constructing controlled drug release systems in biomedical devices [22-28]. Among them, hydrophilic matrix tablets composed of hydrophilic polymers are most commonly applied in oral drug delivery. They are characterized by modulating drug release through rapid swelling and slow erosion of the hydrophilic polymers, therefore improving the bioavailability of the drugs [29,30]. Driven by the valuable feature of hydrophilic matrix tablets, we proposed a novel strategy predicated on swelling and erosion mechanisms to engineer drug-releasing UHMWPE with prolonged antibacterial efficacy. Polyethylene oxide (PEO), a hydrophilic polymer with fast hydrating ability and high swelling capacity, was adopted in UHMWPE along with an antibacterial tea polyphenol (epigallocatechin gallate, EGCG as representative). As illustrated in Fig. 1a, PEO and EGCG were uniformly coated on the surface of UHMWPE grains, forming hybrid delivery pathways in the UHMWPE matrix after compression molding. The incorporated PEO hydrated and swelled upon contact with the aqueous medium, generating osmotic pressure that facilitated water uptake and release of the internal EGCG. Furthermore, the slow erosion of PEO extended the release of encapsulated EGCG, promising in prolonging antibacterial performance to combat PJI.

The incorporated PEO serves to encapsulate EGCG flakes and coat EGCG-wrapped UHMWPE, leading to a smoother surface of the wet-mixed granules compared to virgin UHMWPE (Fig. S1 in Supporting information). Because the ether oxygens in PEO exhibit a certain hydrogen bond interaction with phenolic hydroxyls on EGCG [31,32], the interaction tends to agglomerate multiple granules into larger aggregates. The uniformly coated PEO and EGCG then form hybrid pathways between UHMWPE granules under consolidation pressure, as observed *via* optical microscope (OM) (Fig. 1b) and scanning electron microscope (SEM) (Fig. 1c). Compared to EGCG/UHMWPE (P0E6) with uniform EGCG pathway structure, the hybrid pathways containing PEO presents local aggregation with slender channels. This structure enlarged in SEM resembles the pore-throat structure characterized as varicose bodies with narrow throats in sandstone reservoirs, which is favorable for increasing water permeability and diffusion tortuosity [33,34]. The theoretical volume fraction of the hybrid pathway composed of EGCG and PEO is calculated by the mass fraction and density. Due to smaller density of PEO compared to EGCG, the volume fraction of the hybrid pathway increases with increasing PEO concentration (Fig. 1d). Interestingly, the actual pathway area conducted from OM images is much larger, showing a constant value regardless of the PEO and EGCG proportion (Fig. 1e). The enlargement of value might be associated with the pores at the boundary regions between EGCG/UHMWPE granules, which are in turn filled by the incorporated PEO.

The hydrophilic feature of PEO and the unique morphology of the hybrid pathways encouraged us to explore the release behavior of the PEO/EGCG/UHMWPE composite, a factor critically influential in the antibacterial properties. As reported previously [21], P0E6 exhibits a pronounced decline in EGCG release rate during the initial 12 h period, subsequently stabilizing at a value lower

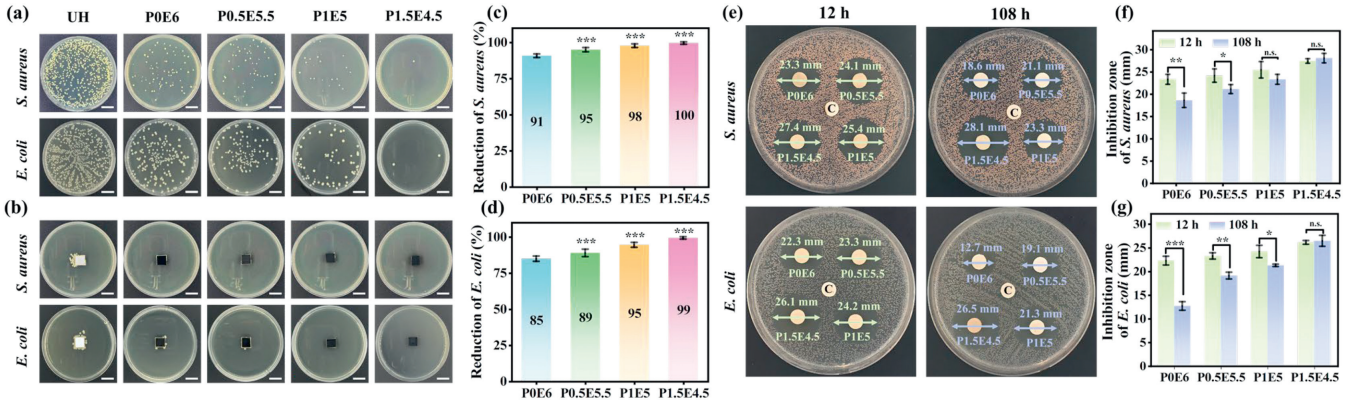

Fig. 2. The antibacterial performance of PEO/EGCG/UHMWPE composites. Photographs of *S. aureus* and *E. coli* (a) co-cultured with and (b) adhered to virgin UHMWPE and PEO/EGCG/UHMWPE composites (scale bar: 1 cm). UH represents UHMWPE. Percentage reduction of (c) *S. aureus* and (d) *E. coli*. Data are presented as mean ± SD ($n = 5$). $^{***}P < 0.001$ *vs.* P0E6. (e) Inhibition zones against *S. aureus* and *E. coli* co-cultured of drug-sensitive tablets soaked in EGCG extracts collected at 12 h and the subsequent 108 h. C represents drug-sensitive tablets without EGCG extracts. Quantitative analysis of the inhibition zones of (f) *S. aureus* and (g) *E. coli*. Data are presented as mean ± SD ($n = 3$). $^{*}P < 0.05$, $^{**}P < 0.01$, $^{***}P < 0.001$. n.s., no significance.

than 0.1 μg mL^{-1} h^{-1}. Although the overall trend remains consistent, it is notable that both the initial and steady-state release rates are higher with elevation in PEO and reduction in EGCG proportion (Fig. 1f). Correspondingly, PEO/EGCG/UHMWPE composites present higher and sustained cumulative release profiles in contrast to EGCG/UHMWPE counterpart (Fig. 1g). This enhanced release behavior can be attributed to the swelling of PEO and capillary force provided by pore-throat like pathway structures, which play pivotal roles in promoting water absorption [35,36]. Additionally, micropores of swelled PEO are observed on the matrix surface after immersion, indicating the erosion of incorporated PEO (Fig. S2 in Supporting information). Synchronization of swelling and erosion of PEO in the composites leads to the sustained release of EGCG, similar to that in hydrophilic matrix tablets. The cumulative EGCG release concentration was assessed at 12 h and the subsequent 108 h to model acute and chronic infection periods. Comparative analysis demonstrates that the EGCG release concentration of PEO/EGCG/UHMWPE composites exceeds that of counterpart lacking PEO at 12 h (Fig. 1h). Notably, the values of P1E5 and P1.5E4.5 are 1.5 ($P < 0.05$) and 2.8 times ($P < 0.001$) that of P0E6, attributed to the rapid water uptake of PEO. Furthermore, the presence of PEO facilitates internal EGCG release, leading to an augmented cumulative EGCG release concentration over the subsequent 108 h as the PEO proportion increases (Fig. 1i). The release concentrations of P1.5E4.5 is 48.1 μg/mL, representing a 14-fold increase compared to P0E6 ($P < 0.001$). All comparisons point to the fact that hydrophilic PEO assists sustained EGCG release through swelling and erosion.

The EGCG release profiles were fitted to Higuchi, Korsmeyer-Peppas, and Weibull release kinetic models [37-39]. The estimated parameters are summarized in Table S1 (Supporting information). All the groups show poor R^2 except for P1.5E4.5, indicating a departure from perfect Fickian diffusion within the system. It is clear that the release of EGCG is influenced by additional factors of PEO swelling and erosion within PEO/EGCG/UHMWPE composites, effects not accommodated by the Higuchi model. Employing the Korsmeyer-Peppas model with the introduction of power-law exponent (n) demonstrates a notable enhancement in the correlation coefficient ($R^2 > 0.90$) across all groups. Although $n \leq 0.5$ demonstrates a predominantly Fickian diffusion mechanism, the increase of n and dissolving-erosion constant K value implies the swelling and erosion process. Weibull approach adapted to complex dissolution and release has the best fit in all scenarios with $R^2 > 0.99$. The extended time scale (a) further underscores the swelling of PEO.

The short-term antibacterial efficacy of PEO/EGCG/UHMWPE composites was initially evaluated through a 12 h bacterial co-culture. The increase of PEO causes a significant decrease in both *S. aureus* and *E. coli* bacterial colonies, regardless of the reduced incorporation of EGCG (Fig. 2a). Among the composites, P1.5E4.5 exhibits minimal bacterial presence, aligning with its superior release performance. Following rinsing planktonic bacteria on the composite surface, bacterial colonies were further co-cultured to determine the presence of any surviving adherent bacteria (Fig. 2b). Bacterial proliferation is constrained yet observable on UHMWPE and P0E6. Few bacterial colonies proliferate with the PEO/EGCG/UHMWPE composite, indicating that the adherent bacteria are deactivated by the gradual release of encapsulated EGCG during PEO swelling and erosion. The statistical results validate the effective antibacterial properties of the composites against both *S. aureus* and *E. coli* (Figs. 2c and d). Since *S. aureus* is more sensitive to EGCG [40], the composites show higher antibacterial effect on *S. aureus* compared to *E. coli*. Notably, the P1.5E4.5 achieves a 100% reduction for both strains within the short-term period, showcasing promise in addressing acute infections.

To assess the sustained antibacterial performance of the composite, the inhibition zone test was conducted on the EGCG release solutions obtained during both the rapid and stable release periods. As depicted in Fig. 2e, all composites yield good antibacterial effects during the 12 h release period. However, the inhibition zones of composites containing PEO are significantly larger than the EGCG/UHMWPE counterpart for the subsequent 108 h release. Based on the statistical analyses (Figs. 2f and g), it is evident that P0E6 experiences a significant decrease in the inhibition zone diameter, aligned with the reduced EGCG release (Figs. 1h and i). The variance in the inhibition zone diminishes with increasing PEO content, signifying the role of PEO in prolonging the antibacterial effect.

The surface-attached bacterial morphology was observed *via* SEM. Fig. 3a illustrates densely aggregated clusters of *S. aureus* with typical spherical shapes on the surfaces of virgin UHMWPE and P0E6. Conversely, isolated bacteria can be observed on the surface of composites containing PEO. The close inspection reveals that the cell walls of *S. aureus* exhibit structural integrity on virgin UHMWPE, yet notable distortion and irregularity with the composites. It manifests as perforations that result in intracellular substance leakage and bacterial folding. Furthermore, *S. aureus* colonies co-cultured with P1.5E4.5 show abnormal cell rupture, seen as complete lysis (arrow in enlarged view). *E. coli* colonies

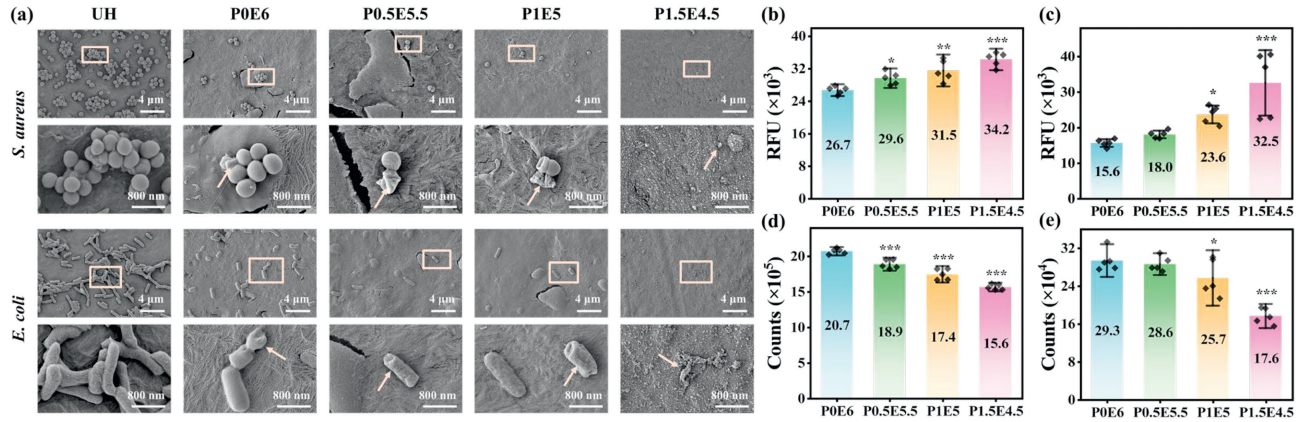

Fig. 3. The antibacterial mechanism of PEO/EGCG/UHMWPE composites. (a) Morphological observation of *S. aureus* and *E. coli* on the surface of virgin UHMWPE and PEO/EGCG/UHMWPE composites. UH represents UHMWPE. Intracellular ROS of the (b) *S. aureus* and (c) *E. coli* after 8 h incubation. Quantitative analysis of the intracellular ATP of (d) *S. aureus* and (e) *E. coli* after 12 h incubation. Data are presented as mean ± SD ($n = 5$). $^{*}P < 0.05$, $^{**}P < 0.01$, $^{***}P < 0.001$. RFU, relative fluorescence units.

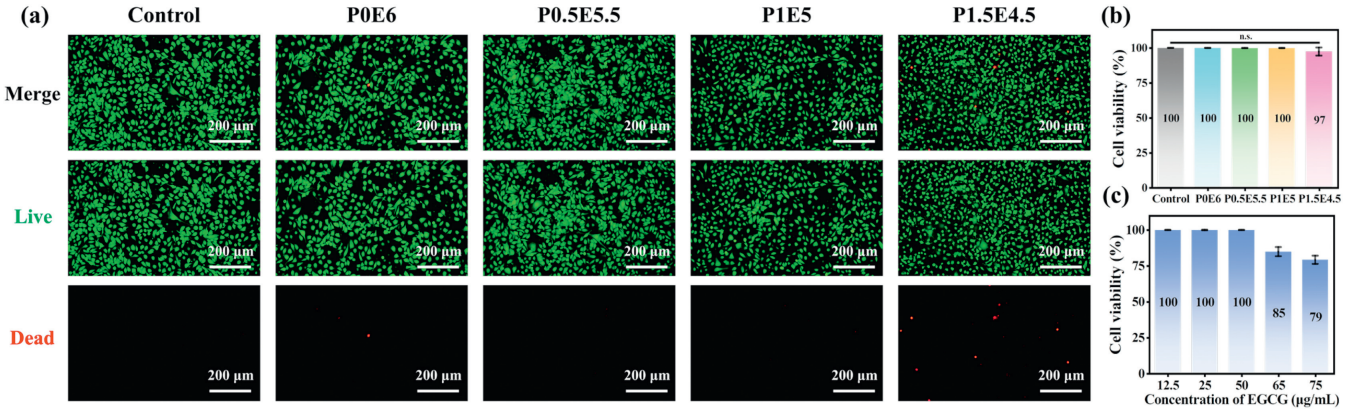

Fig. 4. Cytotoxicity of PEO/EGCG/UHMWPE composites. (a) Live/dead staining images of HUVECs on PEO/EGCG/UHMWPE composites. (b) Quantitative analysis of live/dead staining images. (c) Viability of HUVECs co-cultured with virgin EGCG at different concentrations. Data are presented as mean ± SD ($n = 5$).

display characteristic rod-shaped morphologies with flagella and intact cellular walls. The morphological deformation pattern observed in these colonies is similar to *S. aureus* when cultured with the composites.

Due to the damaging effect of reactive oxygen species (ROS) on the bacterial cell membranes [41], intracellular ROS of the two strains was measured by fluorescence spectrophotometry to determine if the additional PEO affects the ability of EGCG to increase oxidative stress in bacteria. Fluorescence images confirm an 8 h culture period to be the best condition with the highest fluorescence brightness of ROS (Fig. S3 in Supporting information). In this condition, ROS production of bacteria increases with increasing PEO in the composites (Figs. 3b and c), confirming that the augmented release of EGCG in PEO/EGCG/UHMWPE composites is more efficacious in inducing bacterial death. Specifically, the intracellular ROS of *S. aureus* and *E. coli* for P1.5E4.5 is 1.3 and 2 times ($P < 0.001$) of P0E6.

Adenosine triphosphate (ATP) serves as a nucleotide that provides energy for sustaining bacterial activity, the reduction of which signifies cytolysis of the bacteria cells [42]. The luminescence spectra of intracellular ATP reveal a peak luminescence at 570 nm with a half-bandwidth of 82 nm (Figs. S4a and b in Supporting information). The observed decrease in signal counts relative to increased PEO proportion is attributed to the electric charge or group binding effect of the released EGCG (Figs. 3d and e), which causes damage to the bacterial cell membrane [43]. Especially, the electric charge effect contributes significantly, rendering *S. aureus* more susceptible than *E. coli*, as evidenced in Fig. 2.

In light of the essential biosafety and mechanical requirements for implants, there is significant apprehension regarding the cytotoxicity, mechanical strength, and toughness of PEO/EGCG/UHMWPE composites. Fig. 4a illustrates the comprehensive coverage of live cells (depicted in green), with an absence of evident dead cells across all groups. Based on the cell distribution, it can be deduced that the cells are uniformly dispersed across the surface. The viability of human umbilical vein endothelial cells (HUVECs) on the surfaces of all groups surpasses 97%, as depicted in Fig. 4b. Despite the favorable biocompatibility of the composites, heightened concentrations of EGCG reduce the cell viability (Fig. 4c). Therefore, the PEO incorporating proportion is limited to 1.5wt% with a maximum EGCG release concentration of 66.7 ± 12.6 μg/mL (Fig. 1). In terms of mechanical properties, the incorporated PEO results in a moderate decrease in ultimate tensile strength (UTS), work-to-failure and impact strength (Is) (Fig. S5 and Table S2 in Supporting information), presumably due to the hydrophilic PEO affect interfacial adhesion or some solubility in the UHMWPE matrix. Intriguingly, P1E5 presents an enhanced elongation at break (EAB) with a rough fracture surface and obvious load-bearing fibers (Fig. S6 in Supporting information), relevant to the relatively uniform distribution of PEO as observed in OM and SEM (Fig. 1). Nevertheless, all composites with a UTS above 30 MPa, EAB above 250% and Is above 25 kJ/m^2 can be used as clinically validated [44].

Overall, a long-term antibacterial UHMWPE artificial joint material was developed by incorporating hydrophilic PEO to assist the release of EGCG *via* a swelling and erosion mechanism. The

morphology of the PEO/EGCG/UHMWPE composites showed hybrid delivery pathways with a pore-throat like structure, effectively extending EGCG release by enhancing water permeability and diffusion tortuosity. The release kinetics closely aligned with the Korsmeyer-Peppas and Weibull models, substantiating the significant role of PEO in swelling and erosion processes. The antibacterial efficiency of the PEO/EGCG/UHMWPE composites was enhanced 2–3 times with increasing PEO proportion and EGCG release, which was corroborated through segmented release and antibacterial assessments. Given that the incorporated PEO negligibly influences the antibacterial mechanism of released EGCG and the biocompatibility along with mechanical properties of the material, the PEO/EGCG/UHMWPE composites hold considerable promise for manufacturing antibacterial UHMWPE bearing implants with effective long-lasting protection against PJI.

Declaration of competing interest

The authors declare that they have no known competing financial interests or personal relationships that could have appeared to influence the work reported in this paper.

CRediT authorship contribution statement

Yue Ren: Writing – review & editing, Writing – original draft, Funding acquisition, Conceptualization. **Kang Li:** Investigation, Formal analysis, Data curation. **Yi-Zi Wang:** Formal analysis, Data curation. **Shao-Peng Zhao:** Visualization, Software. **Shu-Min Pan:** Validation. **Haojie Fu:** Validation, Investigation. **Mengfan Jing:** Validation, Conceptualization. **Yaming Wang:** Methodology, Conceptualization. **Fengyuan Yang:** Resources, Methodology, Conceptualization. **Chuntai Liu:** Supervision, Project administration.

Acknowledgments

The authors would like to thank the National Natural Science Foundation of China (No. 5220031085), the Postdoctoral Research Project in Henan Province (No. HN2022054), the Key Scientific Research Projects of Colleges and Universities in Henan Province (No. 23A430009), the State Key Laboratory of Polymer Materials Engineering (No. sklpme2022-4-03) and the Key Technologies R&D Program of Henan Province (No. 242102230131). The authors also acknowledge the Laboratory Animal Center of Zhengzhou University and Henan Provincial Key Laboratory of Medical Polymer Materials Technology and Application for kindly providing the biological experimental platform.

Supplementary materials

Supplementary material associated with this article can be found, in the online version, at doi:10.1016/j.cclet.2024.110468.

References

[1] A.B. Anderson, S.E. Slaven, N.L. Watson, et al., JAMA Netw. Open 7 (2024) e2410123.
[2] N.D. Heckmann, J. Yang, K.L. Ong, et al., J. Arthroplasty 39 (2024) 1557–1562.
[3] K. Deere, M.R. Whitehouse, S.K. Kunutsor, et al., Lancet Rheumatol. 4 (2022) e468–e479.
[4] Hip, Knee & Shoulder Arthroplasty: 2023 Annual Report, Australian Orthopaedic Association National Joint Replacement Registry, 2023. https://aoanjrr.sahmri.com/annual-reports-2023.
[5] E.B. Gausden, M.W. Pagnano, K.I. Perry, et al., J. Arthroplasty 36 (2021) 3556–3561.
[6] N. Cortes-Penfield, M. Krsak, L. Damioli, et al., Clin. Infect. Dis. 78 (2024) 188–198.
[7] B.E. Nie, S.C. Huo, X.H. Qu, et al., Bioact. Mater. 16 (2022) 134–148.
[8] X. Li, X. Shu, Y. Shi, et al., Chin. Chem. Lett. 34 (2023) 107986.
[9] V. Sharma, S. Chowdhury, N. Keshavan, et al., Int. Mater. Rev. 68 (2023) 46–81.
[10] E.P.J. Watters, P.L. Spedding, J. Grimshaw, et al., Chem. Eng. J. 112 (2005) 137–144.
[11] R.M. Kumar, P. Gupta, S.K. Sharma, et al., Mater. Sci. Eng. C 77 (2017) 649–661.
[12] R.M. Kumar, K. Rajesh, S. Haldar, et al., J. Drug Deliv. Sci. Technol. 52 (2019) 748–759.
[13] R.M. Kumar, S. Haldar, K. Rajesh, et al., Mater. Sci. Eng. C 105 (2019) 110117.
[14] D. Gil, S. Hugard, N. Borodinov, et al., J. Biomed. Mater. Res. B 111 (2023) 912–922.
[15] S. Lekkala, N. Inverardi, S.C. Grindy, et al., Biomacromolecules 25 (2024) 2312–2322.
[16] D. Gil, A.E. Atici, R.L. Connolly, et al., Bone Joint J. 102b (2020) 151–157.
[17] S. Lekkala, N. Inverardi, J. Yuh, et al., Macromol. Biosci. 24 (2024) 2300389.
[18] Y. Ren, J.C. Lv, S.P. Zhao, et al., Compos. Sci. Technol. 254 (2024) 110689.
[19] F.Y. Wang, Y. Ren, R.T. Lan, et al., Mater. Sci. Eng. C 124 (2021) 112040.
[20] Y. Ren, F.Y. Wang, R.T. Lan, et al., ACS Biomater. Sci. Eng. 7 (2021) 373–381.
[21] Y. Ren, F.Y. Wang, Z.J. Chen, et al., J. Mater. Chem. B 8 (2020) 10428–10438.
[22] J.C. Ye, Y.B. Wang, W.K. Zeng, et al., Adv. Healthcare Mater. 13 (2024) 2300612.
[23] X. Zhang, J. Chen, X. Pei, et al., Chin. Chem. Lett. 35 (2024) 108889.
[24] S. Han, J. Wu, Smart Mater. Med. 5 (2024) 251–255.
[25] C. Xu, Z.Z. Liu, X. Chen, et al., Chin. Chem. Lett. 35 (2024) 109197.
[26] Y. Wu, Z. Wang, Y. Ge, et al., J. Control. Release 370 (2024) 747–762.
[27] Z. Zhang, Z. Hao, C. Xian, et al., Chem. Eng. J. 472 (2023) 145061.
[28] Y. Chen, G. Wang, F. Zhou, et al., Chin. Chem. Lett. (2024), doi:10.1016/j.cclet.2024.110053.
[29] K. Mukherjee, P. Dutta, T.K. Giri, Int. J. Biol. Macromol. 232 (2023) 123448.
[30] M. Cerea, A. Maroni, L. Palugan, et al., J. Control. Release 325 (2020) 72–83.
[31] K. Kim, M. Shin, M.Y. Koh, et al., Adv. Funct. Mater. 25 (2015) 2402–2410.
[32] W. Shim, C.E. Kim, M. Lee, et al., J. Control. Release 307 (2019) 413–422.
[33] J. Lai, G.W. Wang, Z.Y. Wang, et al., Earth Sci. Rev. 177 (2018) 436–457.
[34] R. Yang, Q.H. Hu, S. He, et al., Mar. Pet. Geol. 89 (2018) 415–427.
[35] T. Tajiri, S. Morita, R. Sakamoto, et al., Int. J. Pharm. 395 (2010) 147–153.
[36] Y. Li, Y. Zhao, J. Bi, et al., Constr. Build. Mater. 425 (2024) 136028.
[37] T. Higuchi, J. Pharm. Sci. 52 (1963) 1145–1149.
[38] R.W. Korsmeyer, R. Gurny, E. Doelker, et al., Int. J. Pharm. 15 (1983) 25–35.
[39] F. Langenbucher, J. Pharm. Pharmacol. 24 (1972) 979–981.
[40] Y. Yoda, Z.Q. Hu, T. Shimamura, et al., J. Infect. Chemother. 10 (2004) 55–58.
[41] Y. Cui, Y.J. Oh, J. Lim, et al., Food Microbiol 29 (2012) 80–87.
[42] V.K. Bajpai, A. Sharma, K.H. Baek, Food Control 32 (2013) 582–590.
[43] H. Ikigai, T. Nakae, Y. Hara, et al., Biochim. Biophys. Acta 1147 (1993) 132–136.
[44] A.S.F. Testing, Materials, Standard Specification For Ultra-high-molecular Weight Polyethylene Powder and Fabricated Form For Surgical Implants, ASTM International, 2021 https://www.astm.org/f0648-21.html.